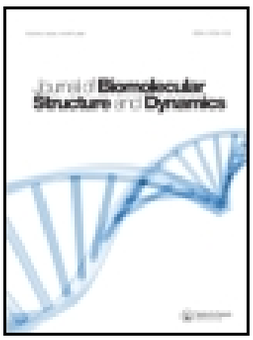

Taylor & Francis
Taylor & Francis Group

Journal of Biomolecular Structure and Dynamics

ISSN: (Print) (Online) Journal homepage: https://www.tandfonline.com/loi/tbsd20

Arylidene analogues as selective COX-2 inhibitors: synthesis, characterization, *in silico* and *in vitro* studies

Dipti L. Namera , Sampark S. Thakkar , Parth Thakor , Umed Bhoya & Anamik Shah

To cite this article: Dipti L. Namera , Sampark S. Thakkar , Parth Thakor , Umed Bhoya & Anamik Shah (2020): Arylidene analogues as selective COX-2 inhibitors: synthesis, characterization, *in silico* and *in vitro* studies, Journal of Biomolecular Structure and Dynamics

To link to this article: https://doi.org/10.1080/07391102.2020.1806109

JOURNAL OF BIOMOLECULAR STRUCTURE AND DYNAMICS
https://doi.org/10.1080/07391102.2020.1806109

Arylidene analogues as selective COX-2 inhibitors: synthesis, characterization, *in silico* and *in vitro* studies

Dipti L. Namera[a], Sampark S. Thakkar[b], Parth Thakor[c], Umed Bhoya[d] and Anamik Shah[a]

[a]Center of Excellence, NFDD Complex, Department of Chemistry, Saurashtra University, Rajkot, Gujarat, India; [b]P.D. Patel Institute of Applied Sciences, Charotar University of Science and Technology, Changa, Gujarat, India; [c]P.G. Department of Biosciences, Sardar Patel University, Vallabh Vidyanagar, Gujarat, India; [d]Department of Chemistry, Saurashtra University, Rajkot, Gujarat, India

Communicated by Ramaswamy H. Sarma

ABSTRACT

Pyrazole derivatives are known to be as non-steroidal anti-inflammatory drugs (NSAID). **Celecoxib** is the pioneer sulfonamide being pyrazole derivative COX-2 inhibitors, which used to treat pain and inflammation; they may also have a role in cancer prevention. In the present investigation, a series of arylidene analogues (**NDP-4011** to **NDP-4016**) were synthesized by the condensation of 4-(3-methyl-5-oxo-4,5-dihydro-1H-pyrazol-1-yl) benzenesulfonamide (**I**) with various substituted aromatic aldehydes in ethanol using a catalytic amount of piperidine. All the synthesized compounds were well characterized by IR, ^{1}H NMR, ^{13}C NMR and mass spectrometry. The cytotoxicity of synthesized compounds was tested on the **NRK-52E** cell line. From which **NDP-4011**, **NDP-4012**, **NDP-4013**, **NDP-1015** and **NDP-4016** were found to have higher cytotoxicity whereas **NDP-4014** showed less cytotoxicity compared to **Celecoxib**. The *in silico* pharmacokinetic parameters of compounds were evaluated to check their candidature as a drug. Molecular docking was carried out on COX-2 structures, which revealed that **NDP-4011** to **NDP-4016** targets allosteric binding site similar to the binding mode of the selective COX inhibitor **Celecoxib**. Furthermore, results of *in vitro* COX-2 inhibition assay supports arylidene analogues as COX-2 inhibitors.

ARTICLE HISTORY

Received 30 April 2020
Accepted 31 July 2020

KEYWORDS

Arylidine; pyrazole; COX-2 enzymes; anti-inflammatory; anti-proliferative

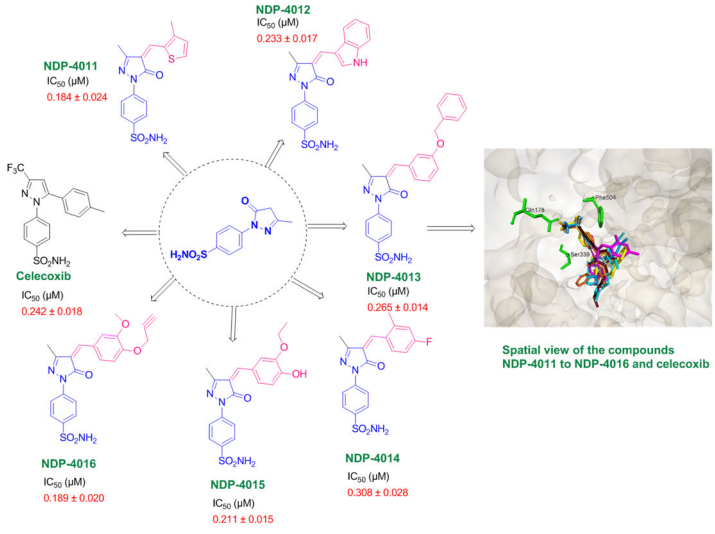

Abbreviations: NSAIDs: non-steroidal anti-inflammatory drugs; COX: cyclooxygenase; PG: prostaglandin; RCSB: Research Collaboratory for Structural Bioinformatics; PDB: Protein Data Bank; NRK-52E: rat kidney epithelial cell line; HBA: hydrogen bond acceptor; HBD: hydrogen bond donor; PSA: polar surface area; PPB: plasma protein binding; MDCK: Madin–Darby Canine Kidney; BBB: blood–brain barrier; ADMET: absorption, distribution, metabolism, excretion, and toxicity; HIA: human intestinal absorbance; DOF: degrees of freedom

CONTACT Dipti L. Namera diptinamera22@gmail.com Center of Excellence, NFDD Complex, Department of Chemistry, Saurashtra University, Rajkot, Gujarat-360005, India

Supplemental data for this article can be accessed online at https://doi.org/10.1080/07391102.2020.1806109.

1. Introduction

Non-steroidal anti-inflammatory drugs (NSAIDs) are frequently used for the treatment of pain and inflammation associated with different diseases, including arthritic disease, chronic pain and menstrual pain (Moodley, 2008). NSAIDs are believed to act through inhibition of cyclooxygenase (COX) enzyme. In the cell, this enzyme is involved in the synthesis of prostaglandins (PGs), which are a key factor of many cellular processes such as inflammation, thromboxanes, angiogenesis and blood clotting. Most of the NSAIDs not only inhibit PGs at the sites of inflammation but also PGs which serve important functions in other parts of the body, a factor which accounts for some of the toxicity of these agents (Vane, 1971). Traditional NSAIDs are non-selective and inhibit both COX-1 and COX-2 enzymes, given that benefits in inflammation, but at the cost of potential opposing effects. However, their chronic use may cause GIT ulceration, bleeding and renal injury (Wolfe et al., 1999). Nowadays, several anti-inflammatory drugs are available in the market but an immense need to develop novel drugs with better safety profile with good efficacy.

The literature survey supports that the ring containing heteroatoms (Doshi et al., 2012, 2015) such as pyrazole and its related analogues represent an important class of heterocycles due to their highly pronounced biological and pharmacological activities (Mariappan et al., 2011; Ramajayam et al., 2010), such as anticancer (Nitulescu et al., 2013), antibacterial (Madhusudana et al., 2017; Mehta et al., 2015; Riyadh, 2011), antiviral (Ouyang et al., 2008), antimalarial (Bekhit et al., 2012), anti-tuberculosis (Karad et al., 2015; Lee et al., 2008) and anti-analgesic (Raga et al., 2013). Some pyrazole compounds have been reported as potential therapeutic agents for the treatment of inflammation (Dekhane et al., 2011; El-Moghazy et al., 2012; Hassan et al., 2019; Ranatunge et al., 2004) by acting on COX enzyme (Mohy El Din et al., 2011). Moreover, sulfonamide being pyrazole compounds have been reported for the treatment of inflammation such as marketed selective COX-2 drug, **Celecoxib** and SC 558 (Chaudhary & Aparoy, 2017; Sakya et al., 2008). A clinical trial of gastrointestinal toxicity with **Celecoxib** vs. other NSAIDs showed that the **Celecoxib** was associated with a lower incidence of symptomatic ulcers and ulcer complications combined, as well as other clinically important toxic effects, compared with NSAIDs at standard dosages (Silverstein et al., 2000).

The use of COX-2 inhibitors are not only anti-inflammatory and analgesics but also used for cancer therapy. A recent study with various malignant tumor cells showed that **Celecoxib** could inhibit the growth of these cells, whereas some of these cancer cells didn't even contain COX-2 (Chuang et al., 2008). Many analogues of **Celecoxib** were generated with small modifications in their chemical structures (Zhu et al., 2002). Some of these analogues retained COX-2 inhibitory activity, whereas many others didn't. However, the ability of all these compounds to kill tumor cells in cell culture was examined. Compound 2,5-dimethyl **Celecoxib**, which possesses the ability to inhibit COX-2 turned out to display stronger anticancer activity than **Celecoxib** itself (Schönthal, 2006) and this anticancer effect could also be verified in highly drug-resistant tumor cells and various animal tumor models (Kardosh et al., 2005; Pyrko et al., 2007).

In the context of the biological importance of COX-2 inhibitor and above-mentioned information reveals the great importance of introducing new selective COX-2 inhibitors which are prototype drugs, its efficiency is comparable to **Celecoxib** and having a lower incidence of side effect. Therefore, we intended to develop a novel approach for structural diversity using different aldehyde and designed and synthesized a series of 4-(substituted phenyl-3-methyl-5-oxo-4,5-dihydro-1-H-pyrazol-1-yl) benzenesulfonamide **NDP-4011** to **NDP-4016** compounds which structurally relates with **Celecoxib**.

In the present study, we tried to synthesis arylidene analogues, which are structurally related to **Celecoxib** (a well-known COX-2 inhibitor). *In silico* molecular docking study and *in vitro* studies revealed that they have tremendous potential as a drug candidate.

2. Materials and methods

Melting points were determined in open glass capillaries and all are uncorrected. Infrared spectra were recorded on a Shimadzu FT-IR-8400 spectrometer using KBr pellet method. ^{1}H NMR and ^{13}C NMR spectra were recorded on a Bruker Advance 400 MHz NMR Spectrometer using DMSO-d_6 as a solvent and TMS as an internal standard. Mass spectra were recorded on the Shimadzu GC-MS-QP-2010 model using the Direct Injection Probe technique. The reaction was monitored by thin-layer chromatography (TLC) on silica gel (Merck 60F_{254}) using (9:1) chloroform-methanol as a solvent system.

2.1. Synthesis of 4-(3-methyl-5-oxo-4,5-dihydro-1H-pyrazol-1yl) benzenesulfonamide (I)

A mixture of 4-hydrazinylbenzenesulfonamide (0.01 mole), methyl acetoacetate and absolute ethanol (15 ml) place in 100 ml round bottom flask, add few drops of hydrochloric acid as a catalyst, the resultant reaction mixture was heated under reflux condition for 18 h. After completion of the reaction as monitored by TLC, the reaction mixture was allowed to cool at room temperature and the formed solid was then filtered by vacuum filtration, washed with cold methanol and dried to give the title product (**I**). Yield (80%); Color: green; M.P.: 204–206 °C; IR (KBr) (cm^{-1}): 3416, 3388, 3078, 2833, 1776, 1681, 1591, 1500, 1460, 1323, 1222, 1159, 1095, 839, 520; MS (m/z): 253 (M); ^{1}H NMR (DMSO-d_6, 400 MHz) δ (ppm): 2.13 (3H, s, -CH_3), 5.43 (1H, s, CH), 7.36 (2H, s, NH_2), 7.86–7.93 (4H, dd, ArH), 11.90(1H, s, OH); ^{13}C NMR (DMSO-d_6) 14.01(CH_3), 43.07(CH_2), 121.24(CH), 121.65(CH), 122.58(CH), 129.64(CH), 138.98(C-S), 144.78(C-N), 149.21(C = N), 171.47(C = O).

2.2. General procedure for the synthesis of derivatives of 4-(substituted phenyl-3-methyl-5-oxo-4, 5-dihydro-1-H-pyrazol-1-yl) benzenesulfonamide (NDP-4011 to NDP-4016)

The mixture of 4-(3-methyl-5-oxo-4,5-dihydro-1*H*-pyrazol-1-yl) benzenesulfonamide (**I**) (0.01 mole) and different aldehydes

(0.01 mole) were taken ethanol using piperidine as a catalyst followed by reflux about 6–8 h. The reaction was monitored by TLC. After completion of the reaction, the reaction mixture was allowed to cool. The precipitate formed upon cooling, was filtered off, and washed with ether and dried in vacuum. Purification of compounds (**NDP-4011** to **NDP-4016**) was carried out by crystallization in methanol.

4-(3-methyl-4-((3-methylthiophen-2-yl)methylene)-5-oxo-4,5-dihydro-1H-pyrazol-1-yl) benzenesulfonamide (**NDP-4011**): R_f: 0.62; Yield (80%); Color: Orange; M.P.: 238–240 °C; IR (cm^{-1}): 3340, 3261, 1676, 1599, 1485, 1305, 1172, 675, 613; MS (m/z): 361 (M+); ^{1}H NMR (DMSO-d_6, 400 MHz) δ (ppm): 2.35 (3H, s, Me), 2.51 (3H, s, Me), 7.19–7.20 (1H, d, C = CH), 7.49 (2H, s, NH_2), 7.60–7.64 (2H, m, ArH), 7.82 (1H, s, ArH), 8.15–8.18 (2H, t, ArH), 8.48 (1H, s, ArH); ^{13}C NMR (DMSO-d_6, 100 MHz) δ (ppm):12.77(CH_2), 14.88(CH_2), 114.50(CH), 119.02(CH), 120.22(CH), 121.03(CH), 129.64(CH), 130.53(CH), 131.17(C), 135.87(CH), 138.54(C-S), 138.60(C-N), 144.76(C = N), 151.80(C), 152.12(C), 162.10(C = O).

4-(4-((1H-indol-3-yl)methylene)-3-methyl-5-oxo-4,5-dihydro-1H-pyrazol-1-yl)benzenesulfonamide (**NDP-4012**): R_f: 0.57; Yield (75%); Color: Light orange; M.P.: 280–282 °C; IR (cm^{-1}): 3265, 3063, 1660, 1591, 1303, 1226, 1120, 736, 592; MS (m/z): 380 (M+); ^{1}H NMR (DMSO-d_6, 400 MHz) δ (ppm): 2.45 (3H, s, Me), 7.32–7.34 (2H, m,ArH), 7.49 (2H, s, NH_2), 7.60–7.65 (2H, m, 2 × ArH, 1 × CH), 8.15 (1H, s, ArH), 8.17–8.18 (1H, d, ArH), 8.29–8.30 (1H, d,ArH), 8.59 (1H, s, ArH), 9.84 (1H, s,ArH), 12.74(1H, s, NH); ^{13}C NMR (DMSO-d_6, 100 MHz) δ (ppm): 13.03(CH_3), 112.45(CH), 113.45(CH), 114.71(CH), 117.68(CH), 118.69(CH), 120.38(CH), 122.26(C), 123.66(CH), 128.12(CH), 129.53(C), 136.44(C-NH), 137.93(C-S), 138.63(CH-NH), 139.09(CH), 144.73(C-N), 151.80(C = N), 163.02(C = O).

4-(3-methyl-5-oxo-4-(3-phenoxybenzylidene)-4,5-dihydro-1H-pyrazol-1-yl)benzenesulfonamide (**NDP-4013**): R_f: 0.60; Yield (72%); Color: Orange; M.P.: 200–202 °C; IR (cm^{-1}): 3375, 3271, 2939, 2874, 1689, 1587, 1550, 1483, 1329, 1249, 1172, 997, 744, 607; MS (m/z): 447 (M+); ^{1}H NMR (DMSO-d_6, 400 MHz) δ (ppm): 2.35 (3H, s, Me), 5.25 (2H, s, CH_2), 7.21–7.24 (2H, d, ArH), 7.47 (2H, s,NH_2), 7.36–7.63 (7H, ArH), 7.80 (1H, s, =CH), 8.17–8.18 (1H, d,ArH), 8.48 (1H, s, ArH), 8.70–8.72 (2H, d, ArH); ^{13}C NMR (DMSO-d_6, 100 MHz) δ (ppm):13.14(CH_3), 69.70(-O-CH_2), 114.91(CH), 115.11(CH), 120.61(CH), 121.20(CH), 121.20(CH), 123.35(CH), 126.22(CH), 127.98(CH), 128.13(CH), 128.51(CH), 129.63(C), 136.20(CH), 136.95(CH), 138.51(C-S), 144.78(C), 148.75(C-N), 152.59(C = N), 162.06(C-O), 162.88(C = O).

4-(4-(4-fluoro-2-methylbenzylidene)-3-methyl-5-oxo-4,5-dihydro-1H-pyrazol-1-yl) benzenesulfonamide (**NDP-4014**): R_f: 0.55; Yield (70%); Color: Orange; M.P.: 218–220 °C; IR (cm^{-1}): 3269, 3068, 2966, 2357, 1722, 1680, 1589, 1485, 1423, 1327, 1163, 1097, 922, 788, 669, 590; MS (m/z): 373 (M+); ^{1}H NMR (DMSO-d_6, 400 MHz) δ (ppm): 2.39 (3H, s, Me), 2.52(3H, s, Me), 7.17–7.22(1H, t, ArH), 7.25–7.28 (1H, dd, ArH), 7.46 (2H, s, NH_2), 7.61–7.63 (2H,d, ArH), 7.94 (1H, s, =CH), 8.09–8.13 (1H, m, ArH), 8.48 (1H, s, ArH), 8.65–8.69 (1H, qt, ArH); ^{13}C NMR (DMSO-d_6, 100 MHz) δ (ppm):13.93(CH_3), 19.67(CH_3), 114.83(CH), 115.60(CH), 117.25(C), 120.56(CH), 121.33(CH), 126.15(CH), 127.51(CH), 129.68(C), 133.08(CH), 134.48(C), 138.27(C-S), 144.82(CH), 145.44(C-N), 152.44(C = N), 161.56(C-F), 167.60(C = O).

4-(4-(3-ethoxy-4-hydroxybenzylidene)-3-methyl-5-oxo-4,5-dihydro-1H-pyrazol-1-yl) benzenesulfonamide (**NDP-4015**): R_f: 0.25; Yield (70%); Color: Orange; M.P.: 208–210 °C; IR (cm^{-1}): 3338, 3277, 3072, 2928, 1724, 1678, 1583, 1448, 1325, 1290, 1136, 1035, 794, 682, 590; MS (m/z): 401 (M+); ^{1}H NMR (DMSO-d_6, 400 MHz) δ (ppm): 1.39–1.43 (3H, t, Me), 2.34 (1H, s, Me),4.12–4.17 (2H, q, CH_2),6.97–6.99 (1H, d,ArH), 7.48 (2H, s, NH_2), 7.63–7.65 (2H, d,ArH), 7.72 (1H, s, =CH), 8.04–8.06 (1H, d, ArH), 8.22–8.25 (1H, m, ArH), 8.41 (1H, s, ArH), 8.72(1H, s, ArH); ^{13}C NMR (DMSO-d_6, 100 MHz) δ (ppm): 13.15(CH_3), 14.62(CH_3), 63.84(CH_2), 115.02(CH), 115.67(CH), 118.22(CH), 120.75(CH), 121.95(CH), 125.29(C),128.63(C), 129.61(CH), 131.26(CH), 138.63(C-S), 144.74(C-N), 146.48(CH), 149.68(C = N), 152.57(C-OH), 153.42(C-O), 162.27(C = O).

4-(4-(3-methoxy-4-(prop-2-yn-1-yloxy)benzylidene)-3-methyl-5-oxo-4,5-dihydro-1H-pyrazol-1-yl) benzenesulfonamide (**NDP-4016**): R_f: 0.37; Yield (65%); Color: Brown; M.P.: 278–280 °C; IR (cm^{-1}): 3317, 3180, 3088, 2976, 1672, 1587, 1500, 1330, 1300, 1159, 993, 738, 615; MS (m/z): 425 (M+); ^{1}H NMR (DMSO-d_6, 400 MHz) δ (ppm): 2.34 (3H, s, Me), 3.88 (3H, s, Me), 4.97(2H, s, CH_2), 7.21–7.22 (1H, d, =CH), 7.49 (2H, s,NH_2), 7.64–8.02 (4H, m, ArH), 8.11–8.21 (2H, d, 2× ArH), 8.41 (1H, s, ArH), 8.74 (1H, s, ArH); ^{13}C NMR (DMSO-d_6, 100 MHz) δ (ppm): 13.14(CH_3), 55.56(CH_3), 56.07(CH_2), 78.51(≡CH), 78.98(≡C), 112.74(CH), 115.05(CH), 116.33(CH), 120.80(CH), 121.26(CH), 123.60(C), 126.93(C), 129.63(CH), 130.09(CH), 138.49(C-S), 144.75(C-N), 148.37(CH), 149.11(C = N), 151.39(C-O), 152.55(C-O), 162.09(C = O).

2.3. *In silico* study

2.3.1. Molecular docking studies

Molecular docking of the protein-ligand complexes was performed with the help of AutoDock 4.2 (Morris et al., 2009). The crystallographic 3D structure of **Celecoxib** bound at the COX-2 active site was downloaded from the RCSB Protein Data Bank (PDB ID: 3LN1) and prepared in AutoDockTools 1.5.6 (Morris et al., 2009) by removal of water and solvent molecules, removal of the bound ligands, the addition of polar hydrogens and partial charge assignment. The prepared structure was saved in AutoDock PDBQT format.

Optimization of all the compounds synthesized (**NDP-4011** to **NDP-4016**) and standard drug (**Celecoxib**) was performed using ChemBio3D Ultra 14.0 (Tiwari et al., 2018). The structure of **NDP-4011** to **NDP-4016** and **Celecoxib** was optimized using the Merck Molecular Force Field (MMFF94) method (Halgren, 1999). The mol2 formats of all ligands were further translated to the PDBQT file using an AutoDockTools 1.5.6. Finally, these ligand models were evaluated for the docking procedure.

Molecular docking was performed to find out the mechanism of binding of the macromolecular targets to small active components. Here, the ligands were docked using the default settings of the Lamarckian genetic algorithm. The AutoGrid dimensions set for receptor were: grid center $X = 31.7241$ Å, $Y = -22.006$ Å, $Z = -17.132$ with the grid size $X = 30$, $Y = 30$,

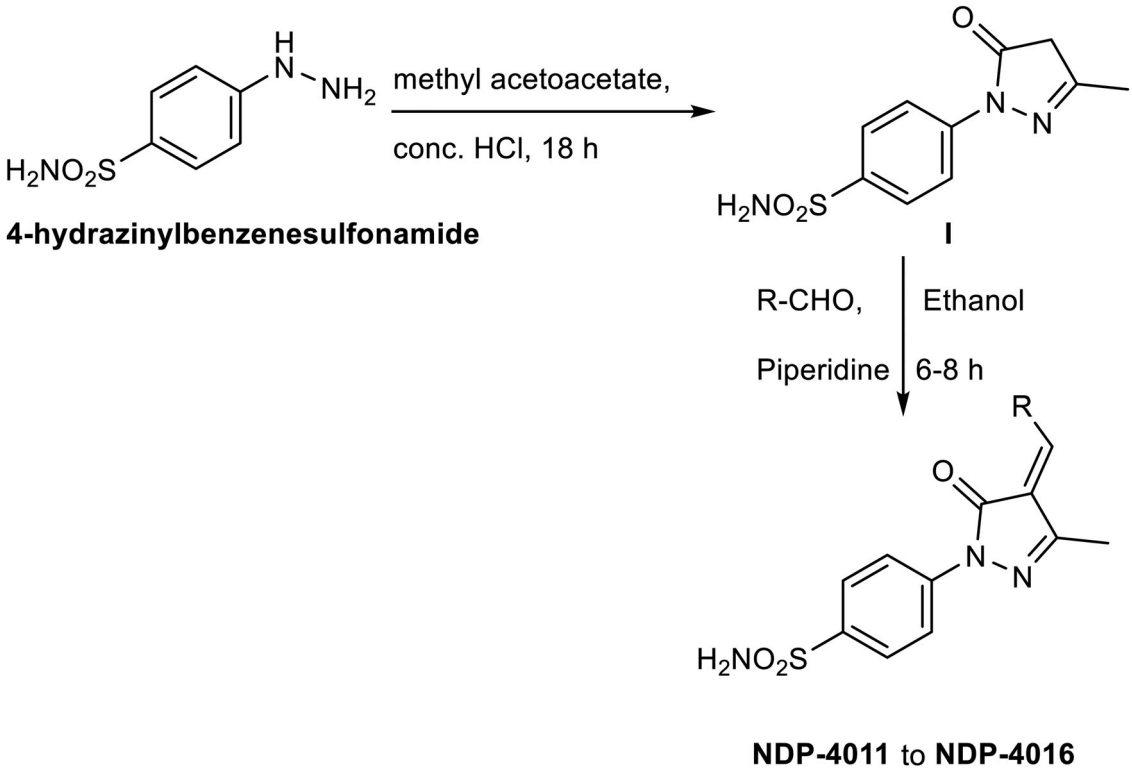

Scheme 1. Synthesis of compounds **I** and **NDP-4011** to **NDP-4016**.

$Z = 30$ and grid spacing: 0.375 Å (Shrivastava et al., 2017). The results were quantified in terms of free binding energy. Biovia Discovery Studio Visualizer v20.1.0.19295 used to find the type of bond with different amino acids and the distance between particular atom/molecule to the amino acids.

2.3.2. Pharmacokinetics evaluation

The pharmacokinetic profile of the compounds (**NDP-4011** to **NDP-4016**) and **Celecoxib** was predicted by using a program VlifeMDS 4.6 (VLife Sciences, Pune, India) software and PreADMET (https://preadmet.bmdrc.kr/) online tool. The program computes pharmacokinetic properties such as Lipinski's Rule of Five, octanol/water partitioning coefficient, aqueous solubility and others.

2.4. Anti-proliferative activity

2.4.1. Cell lines and culture conditions

Rat kidney epithelial cell line (**NRK-52E**) was procured from NCCS, Pune, India. A passage number of 19–25 was used in the present study. The cell line was maintained as a monolayer in Dulbecco's modified Eagle's medium (with 4 mM L-glutamine, 1.5 g/L sodium bicarbonate and 4.5 g/L glucose) containing 10% fetal bovine serum (Gibco, Invitrogen, CA, USA), 50 U/ml penicillin, 50 µg/ml (streptomycin) at 37 °C in a humidified atmosphere of 5% CO_2/95% air.

2.4.2. MTT assay

For cell viability analysis, 10,000 cells/well of rat kidney epithelial cells (**NRK-52E**) were seeded in 96 well culture plates and allowed to grow for 24 h. After 24 h, cells were treated with the various concentrations of synthesized compounds (**NDP-4011** to **NDP-4016**) dissolved in a molecular grade DMSO to find out appropriate IC_{50} value of the respective compounds. The next day, 10 µl of MTT was added to each well and incubated for 3–4 h in a CO_2 incubator at 37 °C. The volume of culture was 100 µl in each well. After the incubation period, the culture medium was removed and the purple crystals formed were dissolved in 100 µl of molecular grade DMSO. The absorbance was recorded with the help of a microplate reader (PromegaGlowmax, USA) at 570 nm (Thakor, Song, et al., 2017; Thakor, Subramanian, et al., 2017).

2.5. Cyclooxygenase (COX-2) inhibition assay

The inhibitory effects of arylidene analogues and **Celecoxib** on COX-2 (human recombinant) were studied by commercial colorimetric COX inhibitor screening assay kit (Cayman test kit-560131; Cayman Chemical Company). Briefly, 160 µl of assay buffer, 10 µl of heme, 10 µl of COX-2 enzyme and 10 µl of arylidene analogues and standard drug (**Celecoxib**) were added into 96-well plate. The plate was shaken for 20 s on a shaker followed by incubation at 25 °C for 5 min. 10 µl of arachidonic acid was added to initiate the reaction. After careful shaking, it was incubated at 25 °C for 10 min. The absorbance of each well was measured at 590 nm with a microplate reader.

3. Results and discussion

3.1. Chemistry

The synthetic route used to synthesize diversified arylidene analogues **NDP-4011** to **NDP-4016** is outlined in Scheme 1.

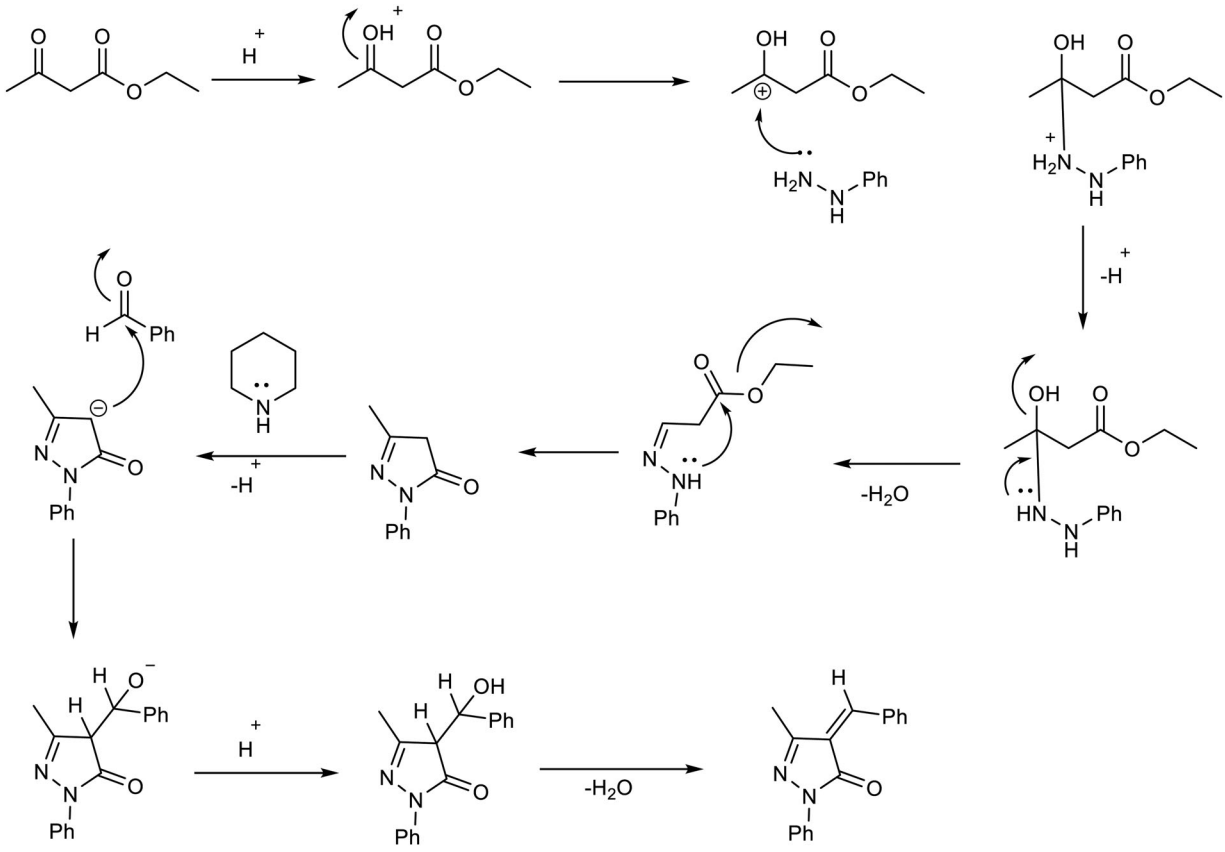

Scheme 2. Proposed mechanism for the formation of **NDP-4011** to **NDP-4016** compounds.

The starting material 4-(3-methyl-5-oxo-4,5-dihydro-1*H*-pyrazol-1-yl) benzenesulfonamide (**I**) was synthesized by the reaction of 4-hydrazinyl benzenesulfonamide with methyl acetoacetate using few drops of concentrated HCl as a catalyst. Finally, the base-catalyzed Knoevenagel condensation of compound **I** with a different substituted aldehyde in ethanol containing a catalytic amount of piperidine afforded the targeted arylidene analogues (**NDP-4011** to **NDP-4016**) in good yield (Scheme-2). Spectral data (IR, ^{1}H NMR, ^{13}C NMR and mass spectrometry) of all newly synthesized compounds were in the full agreement with the proposed structure. The IR spectrum of compounds (**NDP-4011** to **NDP-4016**) showed absorption bands at ~3300 and ~3200 cm^{-1} were due to -NH asymmetric and symmetric stretching, respectively. The other characteristic bands may be attributed to the following group vibrations: ~1140 and ~1330 cm^{-1} (S = O symmetric and asymmetric stretching, respectively), ~1570 cm^{-1} (-NH bends), ~3000 and ~790 cm^{-1} (aromatic -CH stretching and bending, respectively). The ^{1}H NMR spectra showed common signals around 7.36 δ, 7.60 δ, 7.86 δ, 8.30 δ and 8.70 δ were due to aromatic protons present in all compounds. The -C = CH-R proton in all arylidene analogues (**NDP-4011** to **NDP-4016**) occurred as singlet around 8.30 δ. The ^{13}C NMR spectra of all synthesized molecules show resonance due to aromatic carbon in the range of 120–140 δ. The carbons of the pyrazole ring were resonated in the expected region (δ 150–160 ppm). The mass spectrum of all arylidene analogues (**NDP-4011** to **NDP-4016**) showed molecular ion peak (M+) corresponding to their respective molecular weights, which additionally confirmed by the molecular framework.

Table 1. IC_{50} values of compounds (**NDP-4011** to **NDP-4016**) and **Celecoxib** obtained from MTT assay.

Compound ID(s)	IC_{50} (mM)
NDP-4011	0.078 ± 0.0010
NDP-4012	0.064 ± 0.0017
NDP-4013	0.160 ± 0.0033
NDP-4014	0.323 ± 0.0026
NDP-4015	0.099 ± 0.0029
NDP-4016	0.062 ± 0.0009
Celecoxib	0.185 ± 0.0011

3.2. *In vitro* anti-proliferative activity

The anti-proliferative activity of compounds (**NDP-4011** to **NDP-4016**) and standard drug (**Celecoxib**) was carried out by MTT assay. The average IC_{50} (mM) values are presented with standard deviation for three independent experiments in Table 1.

The compounds **NDP-4011**, **NDP-4012**, **NDP-4013**, **NDP-1015** and **NDP-4016** were found to have higher cytotoxicity as compared to **Celecoxib** on **NRK-52E** cell line (Table 1). Out of all synthesized compounds, **NDP-4012** attached with 1*H*-indole and **NDP-4016** having 1-methoxy-2-(prop-2-yn-1-yloxy)benzene showed maximum cytotoxicity. While the presence of 3-methyl thiophene in **NDP-4011** and 2-ethoxy phenol in **NDP-4016** slightly reduces the effect. The compound **NDP-4013** [R=(benzyloxy) benzene)] showed more or less inhibitory concentration similar to that of **Celecoxib**. The presence of benzene ring having -CH_3 and -F in **NDP-4014** found to be less potent compared to **Celecoxib** (Table 1).

3.3. *In silico* ADMET study

One of the most important factors for an orally absorbed drug is, how well the drug is absorbed? For that, it has to follow certain parameters like Lipinski's Rule of Five, polar surface area (PSA), etc. In the present study, all compounds were fitted in Lipinski's Rule of Five with molecular weight less than 500 g/mol (Table 2), HBA (hydrogen bond acceptor) less than 10, HBD (hydrogen bond donor) less than 5 and logP values less than 5. The PSA ($\leq$140 Å^2) and an optimal value of rotatable bonds ($\leq$10) had abundant importance in the oral bioavailability of the drug molecules (Dholakia et al., 2018; Karad et al., 2017; Sapariya et al., 2017; Thakkar, Thakor, Doshi, et al., 2017; Thakkar, Thakor, Ray, et al., 2017; Thakor, Song, et al., 2017; Thakor, Subramanian, et al., 2017; Thakor et al., 2020).

The parameters obtained from PreADMET online tool are compared with the results of standard drug **Celecoxib**. In comparison with **Celecoxib**, **NDP-4011**, **NDP-4014** and **NDP-4015** had lower absorption to CNS (Table 3). Also, all analogues **NDP-4011** to **NDP-4016** had higher human intestinal absorption. In the case of %PPB (plasma protein binding), all compounds synthesized were weakly bound compared to **Celecoxib**. Moreover, all molecules **NDP-4011** to **NDP-4016** had more or less the same MDCK permeability. All the synthesized compounds were not violating the rule more than the maximum permissible limits thus the molecules emerge as potent drug candidates with their drug-likeness properties.

3.4. *In silico* and *in vitro* COX-2 study

To know the selectivity of the compounds (**NDP-4011** to **NDP-4016** and **Celecoxib**) as potential COX-2 inhibitors, *in vitro* cyclooxygenase (COX-2) inhibition activity and *in silico* molecular docking study were carried out. Autodock 4.2 software was used to study molecular interactions between active binding sites of the COX-2 protein target and ligands (**NDP-4011** to **NDP-4016** and **Celecoxib**). *In silico* molecular docking of the compounds **NDP-4011** to **NDP-4016** and **Celecoxib** was ranked based on their lowest binding energy involved in the complex formation at the active site and the result obtained as depicted in Table 4. The binding energy of the docked compounds on COX-2 was found in the range of −9.61 to −10.31 kcal/mol. Compound **NDP-4016** was noted to have the best binding energies of −10.31 kcal/mol. Interaction energy for compounds **NDP-4012**, **NDP-4013** and **NDP-4015** showed almost similar binding energies (Table 4). The lower difference in binding energies of compounds evident that all compounds could be used as a selective COX 2 inhibitors.

All the ligands (Figure 1) reside in the receptor pocket with prodigious ease and display enhanced binding affinity as compared to the reference molecule. It was interesting to observe that amino acid residues A:SER339, A:GLN178 and A:PHE504 of the receptor which plays important roles in binding through hydrogen bonds with the legends (Figure 2(A–G)). Furthermore, the scoring function and the number of hydrogen bonding with the surrounding amino acids

Table 2. Molecular properties of **Celecoxib** and synthesized compounds.

Compound ID(s)	NDP-4011	NDP-4012	NDP-4013	NDP-4014	NDP-4015	NDP-4016	Celecoxib
Molecular weight (g/mol)	361.06	380.09	447.13	373.09	401.10	425.10	381.08
HBA	5	4	5	4	6	6	3
HBD	2	3	2	2	3	2	2
RotB	3	3	6	3	5	7	4
logP	2.62	2.64	4.13	2.97	2.61	2.43	3.96
PSA (Å^2)	77.21	86.06	83.42	76.19	99.95	91.32	63.66

Table 3. Prediction of ADMET parameters of **Celecoxib** and synthesized compounds.

Compound ID(s)	NDP-4011	NDP-4012	NDP-4013	NDP-4014	NDP-4015	NDP-4016	Celecoxib
BBB	00.009	00.034	00.082	00.010	00.013	00.059	00.027
$Caco_2$	00.456	00.766	00.787	00.662	00.543	00.743	00.499
%HIA	96.976	92.216	97.488	97.720	94.890	98.107	96.687
%PPB	74.718	88.079	87.368	82.040	70.797	83.503	91.077
MDCK	04.108	07.265	00.091	00.336	02.004	00.082	45.049

Note: BBB (blood–brain barrier) (Malani, Thakkar, Thakur, Dhandhukia, et al., 2016; Malani, Thakkar, Thakur, Ray, et al., 2016): high absorption CNS >2.0, middle absorption CNS 2.0–0.1, low absorption to CNS <0.1; $Caco_2$ (Malani, Thakkar, Thakur, Dhandhukia, et al., 2016; Malani, Thakkar, Thakur, Ray, et al., 2016): high permeability >70, middle permeability 4–70, low permeability <4; %HIA (human intestinal absorbance) (Malani, Thakkar, Thakur, Dhandhukia, et al., 2016; Malani, Thakkar, Thakur, Ray, et al., 2016): well-absorbed compounds 70%–100%, moderately absorbed compounds 20%–70%, poorly absorbed compounds 0%–20%; %PPB (plasma protein binding) (Patel et al., 2017): strongly bound >90%, weakly bound <90%. MDCK (Thakkar, Thakor, Doshi, et al., 2017; Thakkar, Thakor, Ray, et al., 2017): higher permeability >500, medium permeability 25–500, lower permeability <25.

Table 4. Binding energy of compounds **NDP-4011** to **NDP-4016** and **Celecoxib** with receptor **3LN1**.

Compound ID(s)	Binding energy (kcal/mol)	Intermol energy (kcal/mol)	Torsional energy (kcal/mol)
NDP-4011	−10.14	−11.33	1.19
NDP-4012	−9.65	−10.84	1.19
NDP-4013	−9.61	−11.7	2.09
NDP-4014	−9.78	−10.97	1.19
NDP-4015	−9.64	−11.73	2.09
NDP-4016	−10.31	−12.4	2.09
Celecoxib	−10.23	−11.72	1.49

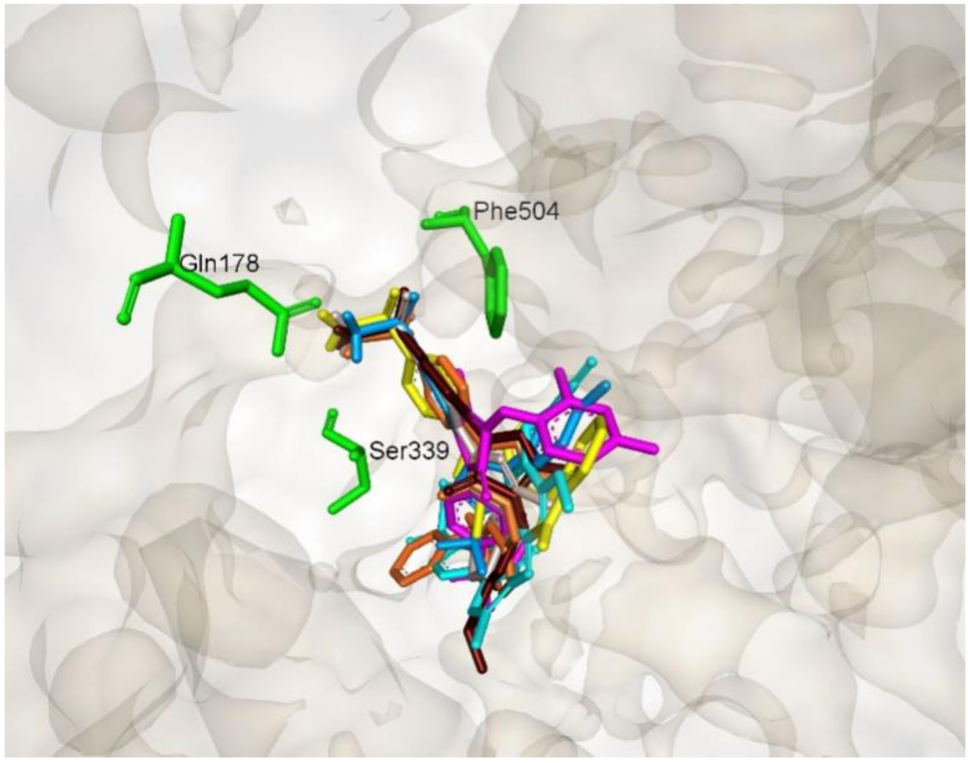

Figure 1. Spatial view of the compounds **NDP-4011** (silver), **NDP-4012** (yellow), **NDP-4013** (orange), **NDP-4014** (purple), **NDP-4015** (brown), **NDP-4016** (sky blue) and **Celecoxib** (blue) bonded in the binding pocket of COX-2 (PDB code: 3LN1). Some important amino acids in the active site bound with compounds **NDP-4011** to **NDP-4016** and **Celecoxib** are shown in this figure for reference.

provided detailed insights into the possible correlation with *in vitro* COX-2 inhibition.

Compounds that showed potent *in vitro* anti-proliferative activity (Table 5) and promising binding score (Table 4) were subjected to *in vitro* COX-2 inhibition assay. As presented in Table 6, all compounds (**NDP-4011** to **NDP-4016** and **Celecoxib**) were selected for *in vitro* COX-2 evaluation. IC_{50} (μM) (concentration that causes 50% enzyme inhibition) values were determined. All the compounds exhibited good inhibitory activities against COX-2 (IC_{50} = 0.150–0.308 μM).

Four targeted compounds (**NDP-4011**, **NDP-4012**, **NDP-4015** and **NDP-4016**) were found as potent COX-2 inhibitors compared to **Celecoxib**. Although compounds **NDP-4011**, **NDP-4016** and **Celecoxib** showed almost similar binding energy (Table 4), **NDP-4011** exhibited good COX-2 inhibition potency (Table 6) because of 5 H-bonds formed with A:GLN172 (2.17 Å), A:HIS75 (2.94 Å), A:SER339 (3.09 Å), A:PHE504 (3.14 Å) and A:ARG499 (3.34 Å) amino acid residues inside COX-2 active site (Figure 2(A)). However, compound **NDP-4016** formed the best stable complex with the receptor (Table 4) but showed lower affinity (IC_{50} = 0.189 μM) than **NDP-4011** (Table 6) due to formed less (4) H-bond compared to **NDP-4011** with the receptor (Figure 2(F)). Whereas compounds **NDP-4012** and **NDP-4015** formed 5 and 6 H-bonds with the active site of receptor, respectively, which is higher than the **Celecoxib** (Figure 2(G)) evident that although they formed less stable drug-receptor complex but showed increase COX-2 inhibition potency (Table 6). Similarly, binding energies and the number of hydrogen bonding for **NDP-4013** (−9.61 kcal/mol, 4) and **NDP-4014** (−9.78 kcal/mol, 2) which was less than standard drug **Celecoxib** and hence found weakest COX-2 inhibitors. The binding energy results and number of H-bonding of compounds with the receptor are in good agreement with the experimental biological data.

4. Conclusion

This study focused on evaluating arylidene analogues as a potential COX-2 inhibitor. *In vitro*, anti-proliferative activity indicated that out of the screened inhibitors, five (**NDP-4011** to **NDP-4013**, **NDP-1015** and **NDP-4016**) displayed better activity results than the standard drug **Celecoxib** on **NRK-52E** cell line. Compounds **NDP-4012** attached with 1*H*-indole and **NDP-4016** having 1-methoxy-2-(prop-2-yn-1-yloxy)benzene had a high inhibition potency. The compound **NDP-4014** displayed a poor IC_{50}. The results of pharmacokinetic data suggested that all analogues tended to be considered as a drug candidate. The stability of the drug-receptor complexes proposed that the majority of the synthesized compounds form stable complexes. *In silico* molecular docking, the study reveals that the binding site for arylidene analogues and **Celecoxib** is the same. Moreover, the *in vitro* COX-2 inhibition activity is also quite nearer to each other.

Acknowledgements

Dipti L. Namera is thankful to FIST-DST and SAP-UGC for instrumentation support and MSME Foundation for financial support as a project fellow for 'Facility for Preservation of Molecular Diversity' (FPMD) project.

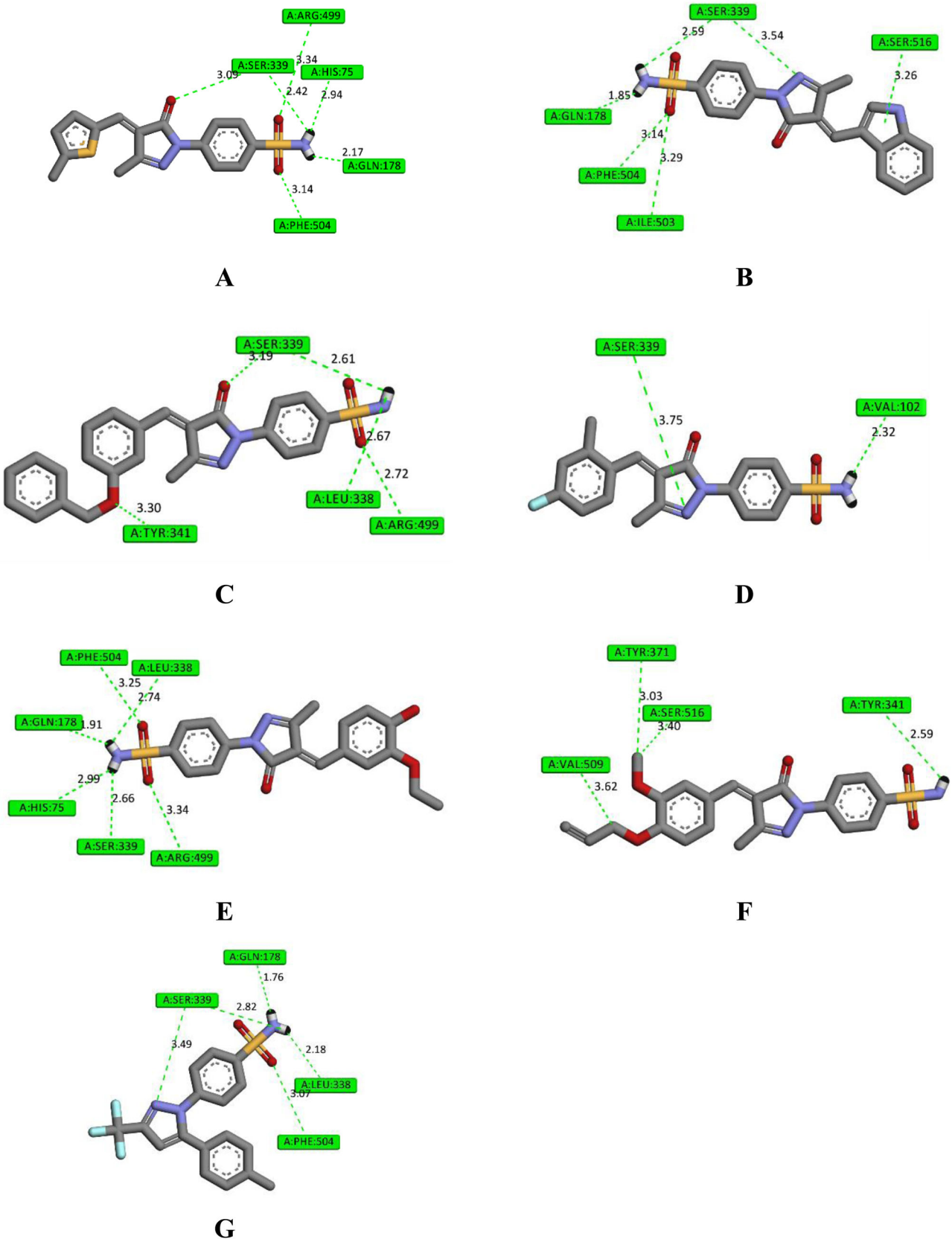

Figure 2. Schematic 2D diagram of H-bond interaction between active site of receptor (3LN1) and (A) **NDP-4011**, (B) **NDP-4012**, (C) **NDP-4013**, (D) **NDP-4014**, (E) **NDP-4015**, (F) **NDP-4015** and (G) **Celecoxib**.

Special thanks to 'National Facility for Drug Discovery through New Chemical Entities (NSE) Development & Instrumentation Support to Small Manufacturing Pharma Enterprises' Programme under and Pharma Research Support (DPRS) jointly funded by Department of Science & Technology, New Delhi, Government of Gujarat Industries Commissionerate & Saurashtra University, Rajkot.

Table 5. Scheme followed to designate the molecules synthesized.

Compound ID(s)	R	Compound ID(s)	R
NDP-4011		**NDP-4014**	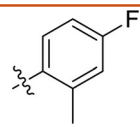
NDP-4012	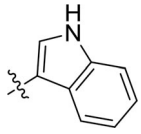	**NDP-4015**	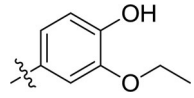
NDP-4013	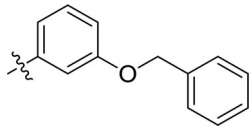	**NDP-4016**	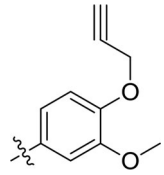

Table 6. COX-2 IC_{50} (μM) values of compounds (**NDP-4011** to **NDP-4016**) and **Celecoxib**.

Compound ID(s)	IC_{50} (μM)
NDP-4011	0.185 ± 0.024
NDP-4012	0.233 ± 0.017
NDP-4013	0.265 ± 0.014
NDP-4014	0.308 ± 0.028
NDP-4015	0.211 ± 0.015
NDP-4016	0.189 ± 0.020
Celecoxib	0.242 ± 0.018

Disclosure statement

The authors declare that they have no conflict of interest.

References

Bekhit, A. A., Hymete, A., & Asfaw, H. (2012). Evaluation of some 1H-pyrazole derivatives as a dual acting antimalarial and anti-leishmanial agents. *Archiv der Pharmazie - Chemistry in Life Sciences*, *345*(2), 147–154. https://doi.org/10.1002/ardp.201100078

Chaudhary, N., & Aparoy, P. (2017). Deciphering the mechanism behind the varied binding activities of COXIBs through molecular dynamic simulations, MM-PBSA binding energy calculations and per-residue energy decomposition studies. *Journal of Biomolecular Structure & Dynamics*, *35*(4), 868–882. https://doi.org/10.1080/07391102.2016.1165736

Chuang, H. C., Kardosh, A., Gaffney, K. J., Petasis, N. A., & Schönthal, A. H. (2008). COX-2 inhibition is neither necessary nor sufficient for celecoxib to suppress tumor cell proliferation and focus formation in vitro. *Molecular Cancer*, *7*, 1–13.

Dekhane, D. V., Pawar, S. S., Gupta, S., Shingare, M. S., Patil, C. R., & Thore, S. N. (2011). Synthesis and anti-inflammatory activity of some new 4,5-dihydro-1,5-diaryl-1H-pyrazole-3-substituted-heteroazole derivatives. *Bioorganic & Medicinal Chemistry Letters*, *21*(21), 6527–6532. https://doi.org/10.1016/j.bmcl.2011.08.061

Dholakia, V., Thakkar, S., Thakkar, A., Doshi, N., & Doshi, H. (2018). Synthesis, characterization, *in silico* studies and *in vitro* antibacterial activity of chromene-fused quinoline analogues. *Madhav Research & Review*, *3*(2), 39–44.

Doshi, H., Bhatt, M., Thakkar, S., & Ray, A. (2012). Synthesis, characterizations and biological screening of tetrahydro-quinazoline analogues. *American Journal of Organic Chemistry*, *2*(5), 122–126. https://doi.org/10.5923/j.ajoc.20120205.03

Doshi, H., Thakkar, S., Khirsariya, P., Thakur, M. C., & Ray, A. (2015). 6-Tosyl-4,5,6,7-tetrahydrothieno[2,3-c]pyridine-3-carboxamide analogues: synthesis, characterization, MO calculation, and antibacterial activity. *Applied Biochemistry and Biotechnology*, *175*(3), 1700–1709. https://doi.org/10.1007/s12010-014-1399-8

El-Moghazy, S. M., Barsoum, F. F., Abdel-Rahman, H. H., & Marzouk, A. A. (2012). Synthesis and anti-inflammatory activity of some pyrazole derivatives. *Medicinal Chemistry Research*, *21*(8), 1722–1733. https://doi.org/10.1007/s00044-011-9691-4

Halgren, T. A. (1999). MMFF VI. MMFF94s option for energy minimization studies. *Journal of Computational Chemistry*, *20*(7), 720–729. https://doi.org/10.1002/(SICI)1096-987X(199905)20:7<720::AID-JCC7>3.0.CO;2-X

Hassan, G. S., Abdel Rahman, D. E., Abdelmajeed, E. A., Refaey, R. H., Alaraby Salem, M., & Nissan, Y. M. (2019). New pyrazole derivatives: Synthesis, anti-inflammatory activity, cycloxygenase inhibition assay and evaluation of mPGES. *European Journal of Medicinal Chemistry*, *171*, 332–342. https://doi.org/10.1016/j.ejmech.2019.03.052

Karad, S. C., Purohit, V. B., Raval, D. K., Kalaria, P. N., Avalani, J. R., Thakor, P., & Thakkar, V. R. (2015). Green synthesis and pharmacological screening of polyhydroquinoline derivatives bearing a fluorinated 5-aryloxypyrazole nucleus. *RSC Advances*, *5*(21), 16000–16009. https://doi.org/10.1039/C5RA00388A

Karad, S. D., Purohit, V. B., Thummar, R. P., Vaghasiya, B. K., Kamani, R. D., Thakor, P., Thakkar, V. R., Thakkar, S. S., Ray, A., & Raval, D. K. (2017). Synthesis and biological screening of novel 2-morpholinoquinoline nucleus clubbed with 1,2,4-oxadiazole motifs. *European Journal of Medicinal Chemistry*, *126*, 894–909. https://doi.org/10.1016/j.ejmech.2016.12.016

Kardosh, A., Soriano, N., Liu, Y. T., Uddin, J., Petasis, N. A., Hofman, F. M., Chen, T. C., & Schönthal, A. H. (2005). Multitarget inhibition of drug-resistant multiple myeloma cell lines by dimethyl-celecoxib (DMC), a non-COX-2 inhibitory analog of celecoxib. Blood, *106*(13), 4330–4338. https://doi.org/10.1182/blood-2005-07-2819

Lee, J. H., Park, H. K., Heo, J., Kim, T., Kim, G. H., Kang, D. H., Song, G. A., Cho, M., Kim, D. S., Kim, H. W., & Lee, C. H. (2008). Drug Rash with Eosinophilia and Systemic Symptoms (DRESS) syndrome induced by celecoxib and anti-tuberculosis drugs. *Journal of Korean Medical Science*, *23*(3), 521–525. https://doi.org/10.3346/jkms.2008.23.3.521

Madhusudana, P., Anuradha, C. M., & Chitta, S. (2017). Design, synthesis, and evaluation of pyrazolo-pyrazole derivatives on Methylisocitratelyase of *Pseudomonas aeruginosa*: *In silico* and *in vitro* study. *Journal of Biomolecular Structure and Dynamics*, *35*(11), 2509–2529. https://doi.org/10.1080/07391102.2016.1223754

Malani, K., Thakkar, S. S., Thakur, M. C., Dhandhukia, P., & Doshi, H. V. (2016). Synthesis, characterization and *in silico* evaluations of diethyl-3-methyl-5-(6-methyl-2-oxo-4-phenyl-1,2,3,4-tetrahydropyrimidine-5-carboxamido) thiophene-2, 4-dicarboxylate analogues as anti-proliferative and anti-microbial agents. *World Journal of Pharmaceutical Sciences*, *4*, 318–330.

Malani, K., Thakkar, S. S., Thakur, M. C., Ray, A., & Doshi, H. (2016). Synthesis, characterization and *in silico* designing of diethyl-3-methyl-5-(6-methyl-2-thioxo-4-phenyl-1,2,3,4-tetrahydropyrimidine-5-carboxamido) thiophene-2,4-dicarboxylate derivative as anti-proliferative and anti-microbial agents. *Bioorganic Chemistry*, *68*, 265–274. https://doi.org/10.1016/j.bioorg.2016.09.001

Mariappan, G., Saha, B. P., Sutharson, L., Singh, A., Garg, S., Pandey, L., & Kumar, D. (2011). Analgesic, anti-inflammatory, antipyretic and toxicological evaluation of some newer 3-methyl pyrazolone derivatives. *Saudi Pharmaceutical Journal*, *19*(2), 115–122. https://doi.org/10.1016/j.jsps.2011.01.003

Mehta, J. V., Gajera, S. B., Thakor, P., Thakkar, V. R., & Patel, M. N. (2015). Synthesis of 1,3,5-trisubstituted pyrazoline derivatives and their applications. *RSC Advances*, *5*(104), 85350–85362. https://doi.org/10.1039/C5RA17185G

Mohy El Din, M. M., Senbel, A. M., Bistawroos, A. A., El Mallah, A., Nour El Din, N. A., Bekhit, A. A., & Abd El Razik, H. A. (2011). A novel COX-2 inhibitor pyrazole derivative proven effective as an anti-inflammatory and analgesic drug. *Basic & Clinical Pharmacology & Toxicology*, *108*(4), 263–273. https://doi.org/10.1111/j.1742-7843.2010.00648.x

Moodley, I. (2008). Review of the cardiovascular safety of COXIBs compared to NSAIDS. *Cardiovascular Journal of Africa*, *19*, 102–107.

Morris, G. M., Huey, R., Lindstrom, W., Sanner, M. F., Belew, R. K., Goodsell, D. S., & Olson, A. J. (2009). AutoDock4 and AutoDockTools4: Automated docking with selective receptor flexibility. *Journal of Computational Chemistry*, *30*(16), 2785–2791. https://doi.org/10.1002/jcc.21256

Nitulescu, G. M., Draghici, C., & Olaru, O. T. (2013). New potential antitumor pyrazole derivatives: synthesis and cytotoxic evaluation. *International Journal of Molecular Sciences*, *14*(11), 21805–21818. https://doi.org/10.3390/ijms141121805

Ouyang, G., Cai, X. J., Chen, Z., Song, B. A., Bhadury, P. S., Yang, S., Jin, L. H., Xue, W., Hu, D. Y., & Zeng, S. (2008). Synthesis and antiviral activities of pyrazole derivatives containing an oxime moiety. *Journal of Agricultural and Food Chemistry*, *56*(21), 10160–10167. https://doi.org/10.1021/jf802489e

Patel, M., Gandhi, P., Thakkar, S., & Doshi, H. (2017). Tetrazolo-quinoxaline analogues as antibacterial agents: Synthesis, characterization and *in silico* ADMET study. *Madhav Research & Review*, *3*(1), 29–36.

Pyrko, P., Kardosh, A., Liu, Y. T., Soriano, N., Xiong, W., Chow, R. H., Uddin, J., Petasis, N. A., Mircheff, A. K., Farley, R. A., Louie, S. G., Chen, T. C., & Schönthal, A. H. (2007). Calcium-activated endoplasmic reticulum stress as a major component of tumor cell death induced by 2,5-dimethyl-celecoxib, a non-coxib analogue of celecoxib. *Molecular Cancer Therapeutics*, *6*(4), 1262–1275. https://doi.org/10.1158/1535-7163.MCT-06-0629

Raga, F. A., Gawad, N. M., Georgey, H. H., & Said, M. F. (2013). Synthesis of novel 1,3,4-trisubstituted pyrazoles as anti-inflammatory and analgesic agents. *European Journal of Medicinal Chemistry*, *63*, 645–654. https://doi.org/10.1016/j.ejmech.2013.03.005

Ramajayam, R., Tan, K. P., Liu, H. G., & Liang, P. H. (2010). Synthesis and evaluation of pyrazolone compounds as SARS-coronavirus 3C-like protease inhibitors. *Bioorganic & Medicinal Chemistry*, *18*(22), 7849–7854. https://doi.org/10.1016/j.bmc.2010.09.050

Ranatunge, R. R., Earl, R. A., Garvey, D. S., Janero, D. R., Letts, L. G., Martino, A. M., Murty, M. G., Richardson, S. K., Schwalb, D. J., Young, D. V., & Zemtseva, I. S. (2004). 3-(2-Methoxytetrahydrofuran-2-yl)pyrazoles: A novel class of potent, selective cyclooxygenase-2 (COX-2) inhibitors. *Bioorganic & Medicinal Chemistry Letters*, *14*(24), 6049–6052. https://doi.org/10.1016/j.bmcl.2004.09.073

Riyadh, S. M. (2011). Enaminones as building blocks for the synthesis of substituted pyrazoles with antitumor and antimicrobial activities. *Molecules*, *16*(2), 1834–1853. https://doi.org/10.3390/molecules16021834

Sakya, S. M., Shavnya, A., Cheng, H., Li, C., Rast, B., Li, J., Koss, D. A., Jaynes, B. H., Mann, D. W., Petras, C. F., Seibel, S. B., Haven, M. L., & Lynch, M. P. (2008). Comparative structure-activity relationship studies of 1-(5-methylsulfonylpyrid-2-yl)-5-alkyl and (hetero)aryl triazoles and pyrazoles in canine COX inhibition. *Bioorganic & Medicinal Chemistry Letters*, *18*(3), 1042–1045. https://doi.org/10.1016/j.bmcl.2007.12.025

Sapariya, N. H., Vaghasiya, B. K., Thummar, R. P., Kamani, R. D., Patel, K. H., Thakor, P., Thakkar, S. S., Ray, A., & Raval, D. K. (2017). Synthesis, characterization, *in silico* molecular docking study and biological evaluation of a 5-(phenylthio) pyrazole based polyhydroquinoline core moiety. *New Journal of Chemistry*, *41*(19), 10686–10694. https://doi.org/10.1039/C7NJ01962A

Schönthal, A. H. (2006). Anti tumor properties of dimethyl-celecoxib, a derivative of celecoxib that does not inhibit cyclooxygenase-2: Implications for glioblastoma therapy. *Neurosurgical Focus*, *20*, 1–10.

Shrivastava, N., Joshi, J., Sehgal, N., & Kumar, I. P. (2017). Cyclooxygenase-2 identified as a potential target for novel radiomodulator scopolamine methyl bromide: An *in silico* study. Informatics in Medicine Unlocked, *9*, 18–25. https://doi.org/10.1016/j.imu.2017.05.007

Silverstein, F. E., Faich, G., Goldstein, J. L., Simon, L. S., Pincus, T., Whelton, A., Makuch, R., Eisen, G., Agrawal, N. M., Stenson, W. F., Burr, A. M., Zhao, W. W., Kent, J. D., Lefkowith, J. B., Verburg, K. M., & Geis, G. S. (2000). Gastrointestinal toxicity with celecoxib vs nonsteroidal anti-inflammatory drugs for osteoarthritis and rheumatoid arthritis: The CLASS study: A randomized controlled trial. Celecoxib Long-term Arthritis Safety Study. JAMA, *284*(10), 1247–1255. https://doi.org/10.1001/jama.284.10.1247

Thakkar, S. S., Thakor, P., Doshi, H., & Ray, A. (2017). 1,2,4-Triazole and 1,3,4-oxadiazole analogues: Synthesis, MO studies, in silico molecular docking studies, antimalarial as DHFR inhibitor and antimicrobial activities. *Bioorganic & Medicinal Chemistry*, *25*(15), 4064–4075. https://doi.org/10.1016/j.bmc.2017.05.054

Thakkar, S. S., Thakor, P., Ray, A., Doshi, H., & Thakkar, V. R. (2017). Benzothiazole analogues: Synthesis, characterization, MO calculations with PM6 and DFT, *in silico* studies and *in vitro* antimalarial as DHFR inhibitors and antimicrobial activities. *Bioorganic & Medicinal Chemistry*, *25*(20), 5396–5406. https://doi.org/10.1016/j.bmc.2017.07.057

Thakor, P., Song, W., Subramanian, R. B., Thakkar, V. R., Vesey, D. A., & Gobe, G. C. (2017). Maslinic acid inhibits proliferation of renal cell carcinoma cell lines and suppresses angiogenesis of endothelial cells. *Journal of Kidney Cancer and VHL*, *4* (1), 16–24. https://doi.org/10.15586/jkcvhl.2017.64

Thakor, P., Subramanian, R. B., Thakkar, S. S., Ray, A., & Thakkar, V. R. (2017). Phytol induces ROS mediated apoptosis by induction of caspase 9 and 3 through activation of TRAIL, FAS and TNF receptors and inhibits tumor progression factor Glucose 6 phosphate dehydrogenase in lung carcinoma cell line (A549). *Biomedicine & Pharmacotherapy*, *92*, 491–500. https://doi.org/10.1016/j.biopha.2017.05.066

Thakor, P., Subramanian, R. B., Thakkar, S. S., & Thakkar, V. R. (2020). Cytotoxic, apoptosis inducing effects and anti-cancerous drug candidature of jasmonates. In K. Saravanan, Chukwuebuka Egbuna, Horne Iona Averal, S. Kannan, S. Elavarasi, & Bir Bahadur (Eds.), *Drug development for cancer and diabetes* (pp. 117–127). Apple Academic Press.

Tiwari, D., Thakkar, S. S., & Ray, A. (2018). Structure-activity relationship in phenothiazine antipsychotic drugs: Molecular orbital calculation, *in silico* molecular docking and physico-chemical parameters. *Indian Journal of Chemistry - Section B*, *57B*, 1194–1202.

Vane, J. R. (1971). Inhibition of prostaglandin synthesis as a mechanism of action for aspirin-like drugs. *Nature: New Biology*, *231*(25), 232–235. https://doi.org/10.1038/newbio231232a0

Wolfe, M. M., Lichtenstein, D. R., & Singh, G. (1999). Gastrointestinal toxicity of nonsteroidal antiinflammatory drugs. *The New England Journal of Medicine*, *340*(24), 1888–1899. https://doi.org/10.1056/NEJM199906173402407

Zhu, J., Song, X., Lin, H. P., Young, D. C., Yan, S., Marquez, V. E., & Chen, C. S. (2002). Using cyclooxygenase-2 inhibitors as molecular platforms to develop a new class of apoptosis-inducing agents. *Journal of the National Cancer Institute*, *94*(23), 1745–1757. https://doi.org/10.1093/jnci/94.23.1745